Decoding across sensory modalities reveals common supramodal signatures of conscious perception

Gaëtan Sanchez[1,2*], Julia Natascha Frey[1,2], Marco Fuscà[2] and Nathan Weisz[1,2]

1 – Paris-Lodron Universität Salzburg, Centre for Cognitive Neuroscience and Division of Physiological Psychology, Hellbrunnerstraße 34, 5020 Salzburg, Austria

2 – Center for Mind/Brain Sciences (CIMeC), University of Trento, via delle Regole 101, 38123 Mattarello (TN), Italy

* Corresponding author: gaetan.sanchez@sbg.ac.at

Keywords

consciousness; perception; near-threshold stimulation; multivariate analysis; decoding analysis; magnetoencephalography

Abstract

An increasing number of studies point to the role of fronto-parietal brain structures in mediating conscious sensory experience. While a majority of studies have been performed in the visual modality, it is implicitly assumed that similar processes are involved in different sensory modalities. However, the existence of supramodal neural processes related to conscious perception has not been convincingly shown so far. In this study, we aim to directly address this issue by investigating whether neural correlates of conscious perception in one modality can predict conscious perception in a different modality. We presented participants with successive blocks of near-threshold tasks involving tactile, visual or auditory stimuli during the same magnetoencephalography (MEG) acquisition. Using decoding analysis in the post-stimulus period between sensory modalities, we uncovered supramodal spatio-temporal neural activity patterns predicting the presence of conscious perception of the feeble stimulation. Interestingly, these supramodal patterns included late activity in primary sensory regions not directly relevant to the task (e.g. neural activity in visual cortex predicting conscious perception of auditory near-threshold stimulation). Our findings reveal for the first time within one experiment a common signature of conscious access across modalities and illustrate the widespread broadcasting of neural representations, even into primary sensory processing regions.

Introduction

While the brain can process an enormous amount of sensory information in parallel, only some information can be consciously accessed, playing an important role in the way we perceive and act in our surrounding environment. An outstanding goal in cognitive neuroscience research is thus to understand the relationship between neurophysiological processes and conscious experiences. Despite tremendous research efforts, however, the precise brain dynamics that enable certain sensory information to be consciously accessed remain unresolved. Nevertheless, progress has been made in research focusing on isolating neural correlates of conscious perception (Crick and Koch, 2003), in particular suggesting that conscious perception - at least if operationalized as reportability (Dehaene and Changeux, 2011) - of external stimuli crucially depends on the engagement of a widely distributed brain network (Naghavi and Nyberg, 2005).

To study neural processes underlying conscious perception, neuroscientists often expose participants to near-threshold (NT) stimuli that are matched to their individual perceptual thresholds (Foley and Legge, 1981; Dagenbach et al., 1989). In NT experiments, there is a trial-to-trial variability in which around 50% of the stimuli at NT-intensity are consciously perceived. Because of the fixed intensity, the physical differences between stimuli within the same modality can be excluded as a determining factor leading to reportable sensation (Ruhnau et al., 2014). However, despite numerous methods used to investigate perceptual consciousness, most neuroscientific studies target a single sensory modality. In the visual domain, it has been shown that reportable conscious experience is present when primary visual cortical activity extends towards hierarchically downstream brain areas (Lamme, 2006), requiring the activation of frontoparietal regions in order to become fully reportable (Dehaene et al., 2006). Nevertheless, a recent MEG study using a visual masking task revealed early activity in primary visual cortices as the best predictor for conscious perception (Andersen et al., 2016). Other studies have shown that neural correlates of auditory consciousness relate to the activation of fronto-temporal rather than fronto-parietal networks (Brancucci et al., 2014; Joos et al., 2014). Additionally, recurrent processing between primary, secondary somatosensory and premotor cortices have been suggested as potential neural signatures of tactile conscious perception (Auksztulewicz et al., 2012; Auksztulewicz and Blankenburg, 2013). Indeed, recurrent processing between higher and lower order cortical regions within a specific sensory system is theorized to be a sufficient marker of conscious processing (Lamme, 2006; Tallon-Baudry, 2012; van Gaal and Lamme, 2012). However, the global workspace framework (Baars, 2005) extended by Dehaene et al. (Dehaene et al., 2014) postulates that the frontoparietal engagement aids in 'broadcasting' relevant information throughout the brain, making it available to various

cognitive modules. In various electrophysiological experiments, it has been shown that this process is relatively late (~300 ms), inducing an increase of the so-called P300 signal (Sergent et al., 2005; Fisch et al., 2009; Melloni et al., 2011). This late brain activity seems to correlate with perceptual consciousness and could reflect the global broadcasting of an integrated stimuli making it conscious. Taken together, theories and experimental findings argue in favor of various 'signatures' of consciousness from recurrent activity within sensory regions to a global broadcasting of information with engagement of fronto-parietal areas. Even though usually implicitly assumed, it is so far unclear whether similar spatio-temporal neural activity patterns are linked to conscious access across different sensory modalities.

In the current study, we investigated conscious perception in different sensory systems using multivariate analysis on MEG data. Our working assumption is that brain activity leading to conscious report is partially independent from the sensory modality and that it instead depends on the common temporal and spatial features of an electrophysiological signal. We hypothesized that processes underlying conscious perception relate to specific spatio-temporal patterns, which allow a decoding of the electrophysiological signal across sensory modalities. The application of multivariate pattern analysis (MVPA) to EEG/MEG measurements offers increased sensitivity in detecting experimental effects distributed over space and time (Cichy et al., 2014, 2015; King and Dehaene, 2014; Tucciarelli et al., 2015; Wutz et al., 2016). MVPA is often used in combination with a searchlight method (Kriegeskorte et al., 2006; Haynes et al., 2007), which involves sliding a small spatial window over the data to reveal areas containing decodable information. The combination of both methods provides spatio-temporal detection of optimal decodability, determining where, when and for how long a specific pattern is present in brain activity. Such multivariate decoding analyses have been proposed as an alternative in consciousness research, complementing other conventional univariate approaches in order to identify neural activity predictive of conscious experience at the single trial level (Sandberg et al., 2014).

Here, we acquired MEG data where each participant performed three different standard NT experiments on three sensory modalities with the aim of characterizing supramodal brain mechanisms of conscious perception. We investigated how single trial neural correlates of perceptual consciousness can be generalized over space and time within and between different sensory systems by using classification analysis on source-level reconstructed brain activity.

Materials and Methods

Participants

Nineteen healthy volunteers with normal or corrected-to-normal vision and no neurological or psychiatric disorders took part in the current study. Of those, three participants were excluded from the analysis due to excessive artifacts in the MEG data leading to an insufficient number of trials per condition after artifact rejection (less than 40 trials for at least one condition). The remaining 16 participants (11 females, mean age: 28.87 years; SD: 3.4 years) reported normal tactile and auditory perception. The ethics committee of the University of Trento approved the experimental protocol, which was used with the written informed consent of each participant.

Stimuli

Auditory stimuli were presented binaurally using MEG-compatible tubal in-ear headphones (SOUNDPixx, VPixx technologies, Canada). Short bursts of white noise with a length of 50 ms were generated with Matlab and multiplied with a Hanning window to obtain a soft on- and offset. Participants had to detect short white noise bursts presented near hearing threshold (Leske et al., 2015). Visual stimuli were Gabor ellipsoid (tilted 45°) back-projected on a translucent screen by a Propixx DLP projector (VPixx technologies, Canada) at a refresh rate of 180 frames per second. The stimuli were presented 50 ms in the center of the screen at a viewing distance of 110 cm. Tactile stimuli were 50 ms stimulation delivered to the tip of the left index finger, using one finger module of a piezo-electric stimulator (Quaerosys, Schotten, Germany) with 2 × 4 rods, which can be raised to a maximum of 1 mm. The module was attached to the finger with tape and the participant's left hand was cushioned to prevent any unintended pressure on the module (Frey et al., 2016). To ensure that the participant did not hear any auditory cues caused by the piezo-electric stimulator during tactile stimulation, binaural white noise was presented during the entire experiment (training blocks included).

Task and design

The participants performed three blocks of a NT perception task. Each block included three separate runs (100 trials each) for each sensory modality, tactile (T), auditory (A) and visual (V). A short break (~1 min) separated each run and longer breaks (~4 min) were provided to the participants after each block. Inside a block, runs alternated in the same order within subject and were pseudo-randomized across subjects (i.e. subject 1 = TVA-TVA-TVA; subject 2 = VAT-VAT-VAT; …). Participants were asked to fixate on a central

white dot in a grey central circle at the center of the screen throughout the whole experiment to minimize eye movements.

In three different training sessions prior to the main experiment, participants' individual perceptual thresholds (tactile, auditory and visual) were determined in the shielded room using a 1-up/1-down staircase procedure. Two randomly interleaved staircases (one up- and one downward) were used with fixed step sizes. A short training run with 20 trials was conducted to ensure that participants had understood the task and to control the accuracy of the threshold measurement.

The main experiment consisted of a detection task (Figure 1A). At the beginning of each run, participants were told that on each trial a weak stimulus (tactile, auditory or visual depending on the run) could be presented at random time intervals. 500 ms after the target stimulus onset, participants were prompted to indicate whether they had felt the stimulus with an on-screen question mark (maximal response time: 2 s). Responses were given using MEG-compatible response boxes with the right index finger and the middle finger. Trials were then classified into hits (detected) and misses (undetected stimulus) according to the participants' answers. Trials with no response were rejected. Catch (above perceptual threshold stimulation intensity) and Sham (absent stimulation) trials were used to control false alarms and correct rejection rates across the experiment. Overall, there were 9 runs with 100 trials each (in total 300 trials for each sensory modality). Each trial started with a variable inter-stimulus interval (1.3–1.8 s, randomly-distributed) followed by an experimental near-threshold stimulus (80 per run), a sham stimulus (10 per run) or a catch stimulus (10 per run) of 50 ms each. Each run lasted for approximately 5 min. The whole experiment lasted for ~1h. The experiment was programmed in Matlab using the open source Psychophysics Toolbox (Brainard, 1997).

MEG data acquisition and preprocessing

MEG was recorded at a sampling rate of 1kHz using a 306-channel (204 first order planar gradiometers, 102 magnetometers) VectorView MEG system (Elekta-Neuromag Ltd., Helsinki, Finland) in a magnetically shielded room (AK3B, Vakuumschmelze, Hanau, Germany). Before the experiment, individual head shapes were acquired for each participant including fiducials (nasion, pre-auricular points) and around 300 digitized points on the scalp with a Polhemus Fastrak digitizer (Polhemus, Vermont, USA). Head positions of the individual relative to the MEG sensors were continuously controlled within a run using five coils. Head movements did not exceed 1 cm within and between blocks.

Data were analyzed using the Fieldtrip toolbox (Oostenveld et al., 2010) and the CoSMoMVPA toolbox (Oosterhof et al., 2016) in combination with MATLAB 8.5 (MathWorks Natick, MA). First, a high-pass filter at 1 Hz (6th order Butterworth IIR) was applied to the

continuous data. Then the data were segmented from 1000 ms before to 1000 ms after target stimulation onset and down-sampled to 512 Hz. Trials containing physiological or acquisition artifacts were rejected. A semi-automatic artifact detection routine identified statistical outliers of trials and channels in the datasets using a set of different summary statistics (variance, maximum absolute amplitude, maximum z-value). These trials and channels were removed from each dataset. Finally, the data were visually inspected and any remaining trials and channels with artifacts were removed manually. Across subjects, an average of 5 channels (± 2 SD) and 8% of trials (± 2.2% SD) were rejected. Bad channels were excluded from the whole data set. Finally, in all further analyses and within each sensory modality for each subject, an equal number of detected and undetected trials was randomly selected to prevent any bias across conditions (Gross et al., 2013).

Source analyses

Neural activity evoked by stimulus onset was investigated by computing event-related fields (ERF). For all source-level analyses, the preprocessed data was 30Hz lowpass-filtered and projected to source-level using an LCMV beamformer analysis (Veen et al., 1997). For each participant, realistically shaped, single-shell headmodels (Nolte, 2003) were computed by co-registering the participants' headshapes either with their structural MRI or – when no individual MRI was available (3 participants) – with a standard brain from the Montreal Neurological Institute (MNI, Montreal, Canada), warped to the individual headshape. A grid with 1.5 cm resolution based on an MNI template brain was morphed into the brain volume of each participant. A common spatial filter (for each grid point and each participant) was computed using the leadfields and the common covariance matrix, taking into account the data from both conditions (detected, undetected) for each sensory modality separately. The covariance window for the beamformer filter calculation was based on 500 ms pre- to 500 ms post-stimulus. Using this common filter, the spatial power distribution was then estimated for each trial separately. The resulting data were averaged relative to the stimulus onset in both conditions (detected and undetected) for each sensory modality, and baseline-normalized relative to a time-window from 200 ms pre-stimulus to stimulus onset. Based on a significant difference between event-related fields of the two conditions over time for each sensory modality, the source localization was performed restricted to specific time-windows of interest. All source images were interpolated from the original resolution onto an inflated surface of an MNI template brain available within the Caret software package (Van Essen et al., 2001). The respective MNI coordinates and labels of localized brain regions were identified with an anatomical brain atlas (AAL atlas; (Tzourio-Mazoyer et al., 2002)) and a network parcellation atlas (Gordon et al., 2016).

Multivariate Pattern Analysis (MVPA) decoding

MVPA decoding was performed for the period 0 to 500 ms after stimulus onset based on normalized (z-scored) single trial source data downsampled to 33Hz (i.e. time steps of 30 ms) without baseline correction. We used multivariate pattern analysis as implemented in CoSMoMVPA (Oosterhof et al., 2016) in order to identify when and what kind of common network between sensory modality is activated during the near-threshold detection task. We defined two classes for the decoding related to the task behavioral outcome (detected (Hit), undetected (Miss)). For decoding within the same sensory modality, single trial source data were randomly assigned to one of two chunks (half of the original data). Data were classified using a 2-fold cross-validation procedure, where a Bayes-Naive classifier predicted trial conditions in one chunk after training on data from the other chunk. For decoding between different sensory modality, single trial source data of one modality were assigned to one testing chunk and the trials from other modalities were assigned to the training chunk. The number of target categories (e.g. detected / undetected) was balanced in each training partition. Training and testing partitions always contained different sets of data. A 'searchlight' analysis defined on each time step and spatial neighborhood structure (source space: 3 cm radius on a 1.5 cm resolution MNI-template grid) provided information about the spatio-temporal loci of classification accuracy. The temporal generalization method was used to explore the ability of each classifier across different time points in the training set to generalize to every time point in the testing set (King and Dehaene, 2014). We generated temporal generalization matrices of task decoding accuracy (detected/undetected), mapping the time at which the classifier was trained against the time it was tested. Generalization of decoding accuracy over time was calculated for all trials and systematically depended on a specific between or within sensory modality decoding. This resulted in a 3x3 design of generalization matrices crossing the factors training/testing and the three sensory modalities. The reported average accuracy of the classifier for each time point and brain region corresponds to the group average of individual effect-size: the ability of classifiers to discriminate 'detected' from 'undetected' trials. We used classification analysis to investigate and robustly identify significant effects across time and brain regions for different sensory modalities.

Statistical analysis

Detection rates for the experimental trials were statistically compared to those from the catch and sham trials, using a dependent-samples T-Test. Concerning the MEG data, the main statistical contrast was between trials in which participants reported a stimulus detection and trials in which they did not (detected vs. undetected).

The evoked response at the source level was tested at the group level for each of the sensory modalities. To eliminate polarity, statistics were computed on the absolute values of source-level event-related responses. Based on the global average of all grid points, we first identified relevant time periods with maximal difference between conditions (detected vs. undetected) by performing group analysis with sequential dependent T-tests between 0 and 600 ms after stimulus onset using a sliding window of 30 ms without overlap. P-values were corrected for multiple comparison using Bonferroni correction. Then, in order to derive the contributing spatial generators of this effect, the conditions 'detected' and 'undetected' were contrasted for the specific time periods with group statistical analysis using nonparametric cluster-based permutation tests with Monte Carlo randomization across grid points controlling for multiple comparisons (Maris and Oostenveld, 2007).

The multivariate searchlight analysis results discriminating between conditions were tested at the group level by comparing the resulting individual accuracy maps against chance level (50%) using a non-parametric approach implemented in CoSMoMVPA (Oosterhof et al., 2016) adopting 10.000 permutations to generate a null distribution. P-values were set at $p<0.05$ for cluster level correction to control for multiple comparisons using a threshold-free method for clustering (Smith and Nichols, 2009), which has been used and validated for MEG/EEG data (Pernet et al., 2015; Turella et al., 2016). The time generalization data were thresholded using a mask with only z-score>3.1 (or $p_{corrected}<0.001$) (see Figure 3A), that is, only 10 out of 10,000 random permutations reached the actual classification accuracies obtained from correctly labeled data. Time points exceeding this threshold were identified and reported for each training data time course to visualize how long time generalization was significant over testing data (see Figure 3B). For visualization purposes, source maps for average decoding accuracy on an inflated brain surface were thresholded to show only grid points with 10% maximum decoding accuracy (Figure 4A; see for a similar approach: (Tucciarelli et al., 2015; Turella et al., 2016)). In order to investigate common patterns of conscious processing between different sensory systems, we performed an intersection analysis. The masking for the intersection analysis (Figure 4B) was performed by taking into account the union of all significant brain grid points (z-score>3.1; or $p_{corrected}<0.001$) for the three symmetric decoding analyses; e.g. when training data come from the visual condition and testing data from the auditory condition, the symmetric decoding analysis is simply the reverse situation. Then, the final mask was restricted to grid points found in all three of these different symmetrical situations (i.e. intersection): visual/auditory, tactile/auditory and visual/tactile.

Results

Behavior

Across all participants (N = 16), detection rates for NT experimental trials were: 55% (SD: 8%) for tactile runs, 50% (SD: 11%) for auditory runs and 56% (SD: 12%) for visual runs. The detection rates for the catch trials were 96% (SD: 5%) for tactile runs, 92% (SD: 11%) for auditory runs and 90% (SD: 12%) for visual runs. The mean false alarm rates in sham trials were 4% (SD: 7%) for tactile runs, 4% (SD: 4%) for auditory runs and 4% (SD: 4%) for visual runs (Figure 1B). Detection rates of NT experimental trials in all sensory modality significantly differed from those of catch trials (tactile: $T_{15} = -20.16$, $p < 0.001$; auditory: $T_{15} = -14.44$, $p < 0.001$; visual: $T_{15} = -9.47$, $p < 0.001$) or sham trials (tactile: $T_{15} = 20.66$, $p < 0.001$; auditory: $T_{15} = 14.66$, $p < 0.001$; visual: $T_{15} = 16.99$, $p < 0.001$) and were comparable to other studies (Leske et al., 2015; Frey et al., 2016).

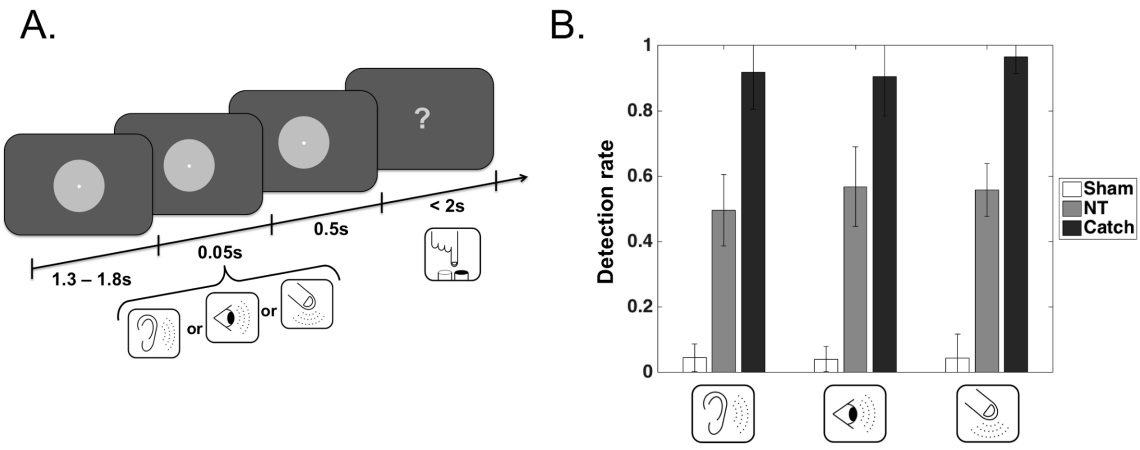

Figure 1. Experimental design and behavioral results. (**A**) After a variable inter-trial interval between 1.3-1.8 s during which participants fixated on a central white dot, a tactile/auditory/visual stimulus (depending on the run) was presented for 50 ms at individual perceptual intensity. After 500 ms, stimulus presentation was followed by an on-screen question mark, and participants indicated their perception by pressing one of two buttons (i.e. stimulation was 'present' or 'absent') with their right hand. (**B**) The group average detection rates for NT stimulation were around 50% across the different sensory modalities. Sham trials in white (no stimulation) and Catch trials in dark (high intensity stimulation) were significantly different from the NT condition in grey within the same sensory modality.

Event-related neural activity

To compare poststimulus processing for 'detected' and 'undetected' trials, evoked responses were calculated at the source level. As a general pattern over all sensory modalities, source-level event-related fields (ERF) averaged across all grid points show that stimuli reported as detected resulted in pronounced post-stimulus neuronal activity, whereas unreported stimuli did not (Figure 2A). ERFs were significantly different over the averaged time-course with specificity dependent on the sensory modality targeted by the stimulation. Auditory stimulations reported as detected elicit significant differences compared to undetected trials first between 190 and 290 ms, and then between 400 and 520 ms after stimulus onset (Figure 2A – top panels). Visual stimulation reported as detected elicits a large increase of ERF amplitude compared to undetected trials from 220-520 ms after stimulus onset (Figure 2A – middle panel). Tactile stimulation reported as detected elicits an early increase of ERF amplitude between 90 and 270 ms then a late activation similar to the auditory modality between 320 and 450 ms after stimulus onset (Figure 2A – bottom panel). Source localization of these specific time periods of interest were performed for each modality (Figure 2B). The auditory condition shows significant early source activity mainly localized to bilateral auditory cortices, superior temporal sulcus and right inferior frontal gyrus, whereas the late significant component was mainly localized to right temporal gyrus, bilateral precentral gyrus, left inferior and superior frontal gyrus. A large activation can be observed for the visual conditions including primary visual areas, cingulate gyrus and a large fronto-parietal network activation. The early contrast of tactile evoked response shows a large difference in the brain activation including primary and secondary somatosensory areas, but also posterior and anterior cingulate gyrus, and a large fronto-parietal network. The late contrast of tactile evoked response presents brain activation including left superior frontal gyrus, right temporal gyrus and right supplementary motor area.

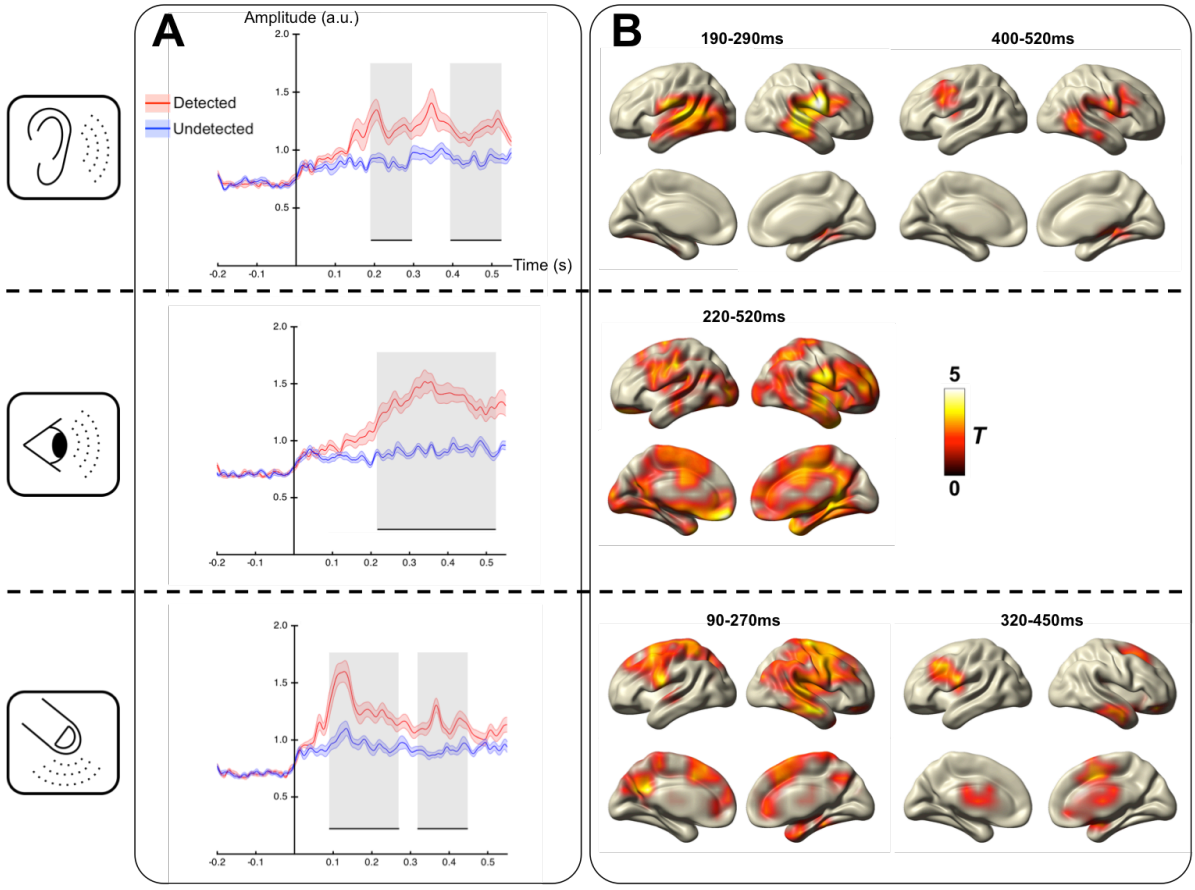

Figure 2. Event-related responses for different sensory modalities: auditory (top panel), tactile (middle panel) and visual (bottom panel). (**A**) Source-level absolute value of group event-related average (solid line) and standard deviation (shaded area) in the detected (red) and undetected (blue) condition for all brain sources. Significant time windows is marked with bottom solid lines (black line: $p_{Bonferroni\text{-}corrected} < 0.05$) for the contrast detected vs. undetected trials. The relative source localization maps are represented in part B for the time period marked by the grey-shaded area. (**B**) Source reconstruction of the significant time period marked in part A for the contrast detected vs. undetected trials, masked at $p_{corrected} < 0.05$. For auditory and tactile conditions the earlier and later significant time periods are represented on the left and the right brain maps, respectively.

Decoding and multivariate searchlight analysis across time

We investigated the generalization of brain activation over time within and between the different sensory modalities. To this end, we performed a spatio-temporal multivariate analysis of reconstructed brain source activity. Time generalization analysis presented as a time-by-time matrix between 0 and 500 ms after stimulus onset shows significant decoding accuracy for each condition (Figure 3A). As can be seen on the black cells located on the diagonal in Figure 3A, cross-validation decoding was performed within the same sensory modality. However, off-diagonal red cells of Figure 3A represent decoding analysis between different sensory modality. Inside each cell, data reported along the diagonal (dashed line) reveal average classifiers accuracy for a specific time point used for the training and testing procedure, whereas off-diagonal data reveal a potential classifier ability to generalize decoding based on different training and testing time points procedure. Indeed, we observed the ability of the same classifier trained on a specific time point to generalize its decoding performance over several time points (see off-diagonal significant decoding inside each cell of Figure 3A). In order to appreciate this result, we computed the average duration of significant decoding on testing time points based on the different training time points (Figure 3B). On average, within the same modalities decoding, the maximum time generalization was found at around 300 ms and we observed maximum classifiers accuracy after this time point (see Figure 3B - top panel).

Early differences specific to the tactile modality have been grasped by the classification analysis by showing high decoding accuracy already at around 90 ms without strong time generalization for this sensory modality, where auditory and visual conditions show only significant decoding starting around 200 ms after stimulus onset. Such an early dynamic specific to the tactile modality could explain off-diagonal accuracy for all between modalities decoding where the tactile modality was involved (Figure 3A). Interestingly, time generalization concerning between sensory modality decoding (red cells in Figure 3A) started later (after 150 ms) compared to within sensory modality decoding, and presented maximal generalization at around 400 ms (see Figure 3B - bottom panel). The time-generalization analysis revealed time-clusters restricted to late evoked responses with maximal decoding accuracy on average after 300 ms for all conditions. The similarity of this time-cluster over all three sensory modalities suggests the unspecificity of such brain activation.

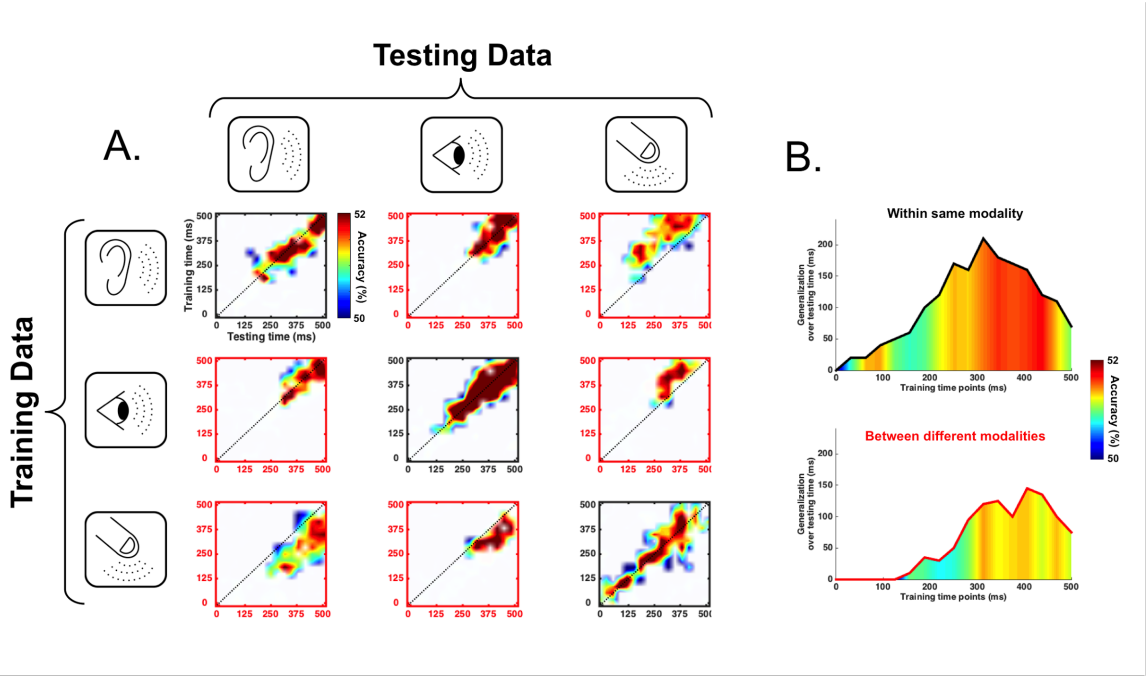

Figure 3. Time-by-time generalization of significant searchlight MVPA decoding within and between sensory modality. 3x3 matrices of decoding results represented over time (from stimulation onset to 500 ms after). **(A)** Each cell presents the result of the searchlight MVPA with time-by-time generalization analysis where classifier accuracy was significantly above chance level (50%) (masked at $p_{corrected}<0.001$). Accuracy is averaged over all significant brain voxels at one specific time point. For each temporal generalization matrix, a classifier was trained at a specific time sample (vertical axis: training time) and tested on all time samples (horizontal axis: testing time). The black dotted line corresponds to the diagonal of the temporal generalization matrix, i.e., a classifier trained and tested on the same time sample. This procedure was applied for each combination of sensory modality, i.e. presented on the first row is decoding analysis performed by classifiers trained on the auditory modality and tested on auditory, visual or tactile (1st, 2nd and 3rd column respectively) for the two classes: detected and undetected trials. The cells contoured with black line axes (on the diagonal) correspond to within the same sensory modality decoding, whereas the cells contoured with red line axes correspond to between different modalities decoding. **(B)** Summary of average time-generalization and decoding performance over time for all within modality analysis (top panel: average based on the 3 blacks cells of part A) and between modalities analysis (bottom panel: average based on the 6 red cells of part A). For each specific training time point on the x-axis the average duration of classifier's ability to significantly generalize on testing time points was computed and reported on the y-axis. Additionally, the average classifiers accuracies over all testing time for a specific training time point is represented as a color scale gradient.

Decoding and multivariate searchlight analysis across space

Restricted to the respective significant time clusters (Figure 3A), we investigated the underlying brain sources resulting from the searchlight analysis within and between conditions (Figure 4A). The decoding within the same sensory modality revealed strong primary sensory cortex involvement for each specific modality condition (see Figure 4A; brain plots on diagonal). For auditory and tactile conditions, the occipital and parietal lobes were involved, respectively, in addition to the putatively task-relevant primary sensory cortices. However, decoding between different sensory modalities restricted to late significant time-clusters revealed fronto-parietal brain regions in addition to diverse primary sensory regions (see Figure 4A; brain plots off diagonal).

Similar regional brain activity was used by the classifiers for all direct symmetrical decoding analyses, for instance with auditory training and a visual testing dataset, and vice versa (all symmetrical cells around the diagonal of Figure 4A). The intersection of brain regions for the three symmetrical situations of between-sensory decoding revealed common network localization independent of a specific sensory modality condition (Figure 4B). This result highlights a brain network that includes frontal and parietal regions, such as inferior frontal and parietal gyrus, but also primary sensory areas related to the task and deep brain structure such as the insula and cingulate cortex (see Table 1). By using a parcellation atlas (Gordon et al., 2016), we depicted regions belonging to different known brain networks including sensory systems, default mode, attentional and fronto-parietal network (Power et al., 2011). Of particular interest with respect to the idea of broadcasting (Dehaene et al., 2006) introduced earlier, is the issue of whether there is a temporal gradient with respect to the decoding across these different neural systems. For this purpose, we computed for each relevant brain voxel the average latency over training-time of significant decoding results at the group level across all between sensory modalities analysis. Regarding between different modalities decoding, primary systems present later significant decoding latency compared to other networks (Figure 5).

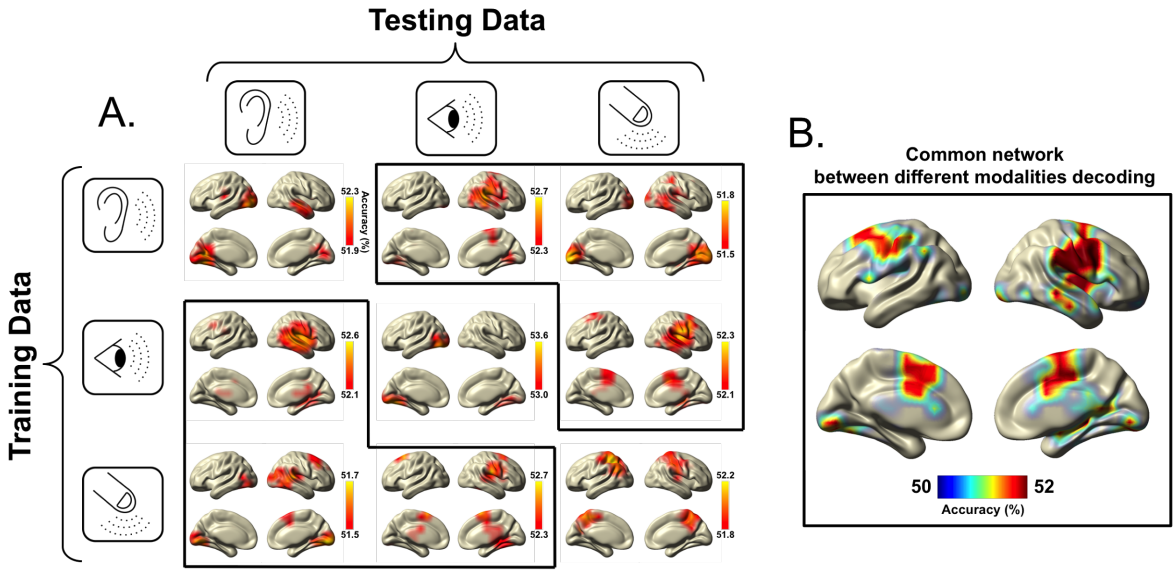

Figure 4. Spatial distribution of significant searchlight MVPA decoding within and between sensory modality. **(A)** Source brain maps for average decoding accuracy restricted to a specific time-generalization significant cluster (cf. Figure 3A). For visualization purpose, brain maps were thresholded for each condition with 10% maximum decoding accuracy (above 90th percentile). **(B)** Accuracy map for the intersection of all significant spatial features involved in detected/undetected decoding analysis based on searchlight MVPA restricted to between sensory modality conditions (intersection of brain maps contoured with black-lines in part A of this figure). First the union of significant brain maps was computed for the three symmetric decoding analysis (i.e. symmetric decoding when training data come from visual and testing data from auditory is simply the reverse situation: 1st column of 2nd row and 2nd column of 1st row). Then, the final mask presented here is restricted to the intersection across these three different symmetrical situations: visual/auditory, tactile/auditory and visual/tactile. The color scale depicts the average accuracy across all between sensory modality and over all specific significant respective time clusters (cf. Figure 3A).

Regions	MNI coordinates X	Y	Z	Latency (ms)	Accuracy
Auditory (Aud)					
- right Heschl gyrus	55	-20	10	382	54,76%
- right superior temporal gyrus	70	-20	10	383	54,99%
Visual (Vis)					
- right lingual gyrus	10	-80	-5	428	54,50%
- left calcarine fissure	-5	-95	-5	397	54,27%
- right inferior occipital gyrus	25	-95	-5	418	54,69%
Somatosensory (Som)					
- right postcentral gyrus	55	-20	40	391	54,96%
Ventral Attention (VenAtt)					
- right inferior frontal gyrus (triangular part)	55	25	10	356	54,57%
Dorsal Attention (DorAtt)					
- left superior frontal gyrus	-20	10	55	344	54,80%
Cingulum Opercularis (CingOp)					
- right inferior frontal gyrus (opercular part)	40	10	10	402	54,66%
- left inferior frontal gyrus (opercular part)	-50	10	10	365	53,86%
- right insula	40	-5	-5	332	54,82%
- right median cingulate	10	10	40	356	54,46%
Default Mode Network (DMN)					
- left inferior parietal	-50	-50	40	357	54,37%
Fronto-Parietal (FrPar)					
- right middle frontal gyrus	40	10	40	380	54,93%
Retrosplenial cortex (Retro)					
- right precuneus	10	-50	10	366	54,64%

Table 1. Common brain regions revealed across all between sensory modalities decoding of conscious perception. This table reports brain regions presented in Figure 4B and sorted according to the network parcellation from (Gordon et al., 2016). For each specific brain region we reported the latency where a significant decoding was found over training time and the maximum classifiers accuracy measures overall significant time clusters across all combination of between sensory modality decoding.

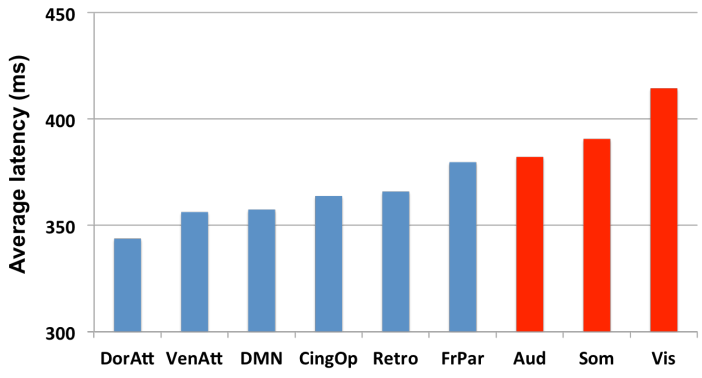

Figure 5. Average significant between sensory modalities decoding latency for each specific network voxels revealed by the intersection analysis. This figure depicts when a decoding analysis across different sensory modalities was found as significant, restricted to brain regions presented in Figure 4B according to relevant specific network labels (see Table 1). Primary sensory systems (red bars) significant decoding appears to be later than other networks (blue bars).

Discussion

We investigated a standard NT experiment targeting three different sensory modalities in order to explore common spatio-temporal brain activity related to conscious perception using multivariate and searchlight analysis. Our findings focusing on the post-stimulus evoked responses are in line with previous studies for each specific sensory modality, showing stronger brain activation when the stimulation was reported as perceived (Karns and Knight, 2008; Leske et al., 2015; Frey et al., 2016). However, the work presented here is the first study, to our knowledge, to provide direct evidence of common electrophysiological correlates of conscious access across sensory modalities by exploiting the advantages of searchlight multivariate analysis decoding with MEG source reconstruction.

Our first results suggest significant temporal and spatial differences when a univariate contrast between 'detected' and 'undetected' trials was used to investigate sensory-specific evoked responses. At the source level, the global group average activity revealed different significant time periods according to the sensory modality targeted where modulations of evoked responses related to detected trials can be observed (Figure 2A). In the auditory and visual modalities, we found significant differences after 200 ms. In the auditory domain, perception- and attention-modulated sustained responses around 200 ms from sound onset were found in bilateral auditory and frontal regions using MEG (Kauramäki et al., 2012; Zoefel and Heil, 2013). Several EEG studies have already shown that evoked responses related to NT visual stimuli revealed an increase in amplitude between 200 and 400 ms, reflecting the so-called P300 modulation (Devrim et al., 1999; Polich, 2007). Using MEG, a previous study confirmed awareness-related effects from 240 to 500 ms after target presentation during visual presentation (Wyart and Tallon-Baudry, 2008). The differences in the transient responses are earlier in the somatosensory domain compared to the other sensory modalities, and have been previously identified using EEG at around 100 and 200 ms (Ai and Ro, 2014). Moreover, previous MEG studies have shown early brain signal amplitude modulation (<200ms) related to tactile perception in NT tasks (Palva et al., 2005; Wühle et al., 2010; Frey et al., 2016). Such neuronal activity involve sensory regions and fronto-parietal brain networks (Palva et al., 2005).

In general, stable characteristics of brain signals have been proposed as a transient stabilization of distributed cortical networks involved in conscious perception (Schurger et al., 2015). Despite similar late brain activation in response to auditory and tactile stimulation, this first analysis can hardly identify common dynamics and network involvement across sensory modality. Interestingly, multivariate decoding analysis was used to refine spatio-temporal similarity across these different sensory systems.

Stability and timing differences of brain activity related to conscious perception across sensory systems have been explored with the time generalization analysis. The presence of similar brain activity can be revealed between modalities using such a technique, even if significant ERF modulation is distributed over time. As expected, tactile diagonal decoding presents significant classification accuracy already around 100 ms after stimulus onset, whereas auditory and visual modalities start to show significant decoding later in time. These results are visible in the cross-validation analysis (diagonal cells of Figure 3A). Moreover, between-modality time-generalization analysis involving tactile runs show off-diagonal significant decoding (Figure 3A). This result suggests the existence of early but similar brain activity patterns related to conscious perception in the tactile domain compared to auditory and visual modalities. Generally, decoding results revealed a significant time cluster after 300 ms with high classifier accuracy that speaks in favor of a late neural response related to conscious report. Note that, as seen also in multiple other studies using decoding (Tucciarelli et al., 2015; Cichy et al., 2016; Turella et al., 2016; Wutz et al., 2016), the average accuracy can be relatively low and yet remains significant at the group level. The rigor of our approach is underlined by the facts that the reported decoding results are restricted to highly significant effects ($P_{corrected}<0.001$; see Methods section) and to the *intersection of all* significant effects between sensory modalities decoding (Figure 4B).

Indeed, we observed the ability of the same classifier trained on specific time points with a specific sensory modality condition to generalize its decoding performance over several time points with the same or another sensory modality. This result speaks in favor of supramodal brain activity patterns that are consistent and stable over time. In addition, the searchlight analysis across brain regions highlighted a common brain network activation during these significant time-generalization clusters. The MVPA searchlight results suggested a common and stable late brain activation related to conscious perception report with strong similarity across all sensory systems tested.

Our results conform to those of previous studies in underlying the importance of late activity patterns as crucial markers of conscious access (Sergent and Dehaene, 2004; Dehaene et al., 2006) and decision-making processes (Polich, 2007; Joos et al., 2014). In this study, we extend the involvement of a parieto-frontal network across three different sensory systems. Some of the brain regions found in our searchlight analysis, namely the superior frontal cortex and left inferior parietal cortex, are shared with other functional brain networks such as the salience network (Kucyi et al., 2012; Chen et al., 2016). These regions have been previously found to be activated by attention-demanding cognitive tasks (Menon and Uddin, 2010). We would like to emphasize that one cannot conclude from our study that the observed supramodal network is exclusively devoted to conscious report. Brain networks identified in this study share common brain regions and dynamics with the attentional and

588 salience networks that remain relevant mechanisms to performing a NT-task. Since sensory
589 modalities are usually interwoven in real life, our findings of a supramodal network that may
590 subserve both conscious access and attentional functions have a higher ecological validity
591 than results from previous studies on conscious perception for single sensory modality.
592 Despite the ongoing debate about the underlying brain generators of the P300, this
593 brain signal remains an important marker of conscious perception across different sensory
594 modalities (Fallgatter et al., 1997; Rutiku et al., 2015). An earlier study combined EEG with
595 fMRI to demonstrate that both techniques indicated nearly the same brain areas involved in
596 the P300 component, i.e. the temporoparietal junctions, supplementary motor areas (SMA),
597 anterior cingulate cortex, insula and medial frontal gyrus (Mulert et al., 2004). Many of the
598 brain areas found in the decoding analysis between sensory modalities overlay the P300
599 related regions, i.e. middle frontal gyrus, inferior parietal gyrus and cingulate cortex (Polich,
600 2007; Joos et al., 2014).
601 Although the integration of classically unimodal primary sensory cortices into a
602 processing hierarchy of sensory information is well established (Felleman and Essen, 1991),
603 some studies suggest multisensory roles of primary cortical areas (Lemus et al., 2010; Liang
604 et al., 2013). Today it remains unknown how such multisensory responses could be related
605 to an individual's unisensory conscious percepts. Interestingly, the intersection analysis
606 revealed that primary sensory regions are strongly involved in all the between sensory
607 modality decoding analysis. This important result suggests that early sensory cortices from a
608 specific modality contain sufficient information to allow the decoding perceptual conscious
609 access in another different sensory modality. In line with the idea of the broadcasting of an
610 integrated conscious percept (Dehaene et al., 2006), these results suggest a late active role
611 of primary cortices over three different sensory systems (Figure 5). One study reported
612 efficient decoding of visual object categories in early somatosensory cortex using fMRI and
613 multivariate pattern analysis (Smith and Goodale, 2015). Another fMRI experiment
614 suggested that sensory cortices appear to be modulated via a common supramodal
615 frontoparietal network, attesting to the generality of attentional mechanism toward expected
616 auditory, tactile and visual information (Langner et al., 2011). However, in our study we
617 demonstrate how local brain activity from different sensory regions reveal a specific dynamic
618 allowing generalization over time to decode the behavioral outcome of a subjective
619 perception in another sensory modality. These results speak in favor of intimate cross-modal
620 interactions between modalities in perception (Pooresmaeili et al., 2014). Finally, our results
621 suggest that primary sensory regions remain important at late latency after stimulus onset for
622 resolving stimulus perception over different sensory modalities. We propose that this
623 network should be more generally cast as enhancing the processing of behaviorally relevant
624 signals, here the sensory targets.

We successfully characterized common patterns over time and space suggesting generalization of consciousness-related brain activity across different sensory NT tasks. To our knowledge, this is the first study to report significant spatio-temporal decoding across different sensory modalities in a near-threshold perception experiment. Indeed, our results speak in favor of the existence of stable and supramodal brain activity patterns, distributed over time and underlying conscious perception processes. The stability of brain activity patterns over different sensory modalities presented in this study is, to date, the most direct evidence of a common network activation leading to conscious access (Dehaene and Changeux, 2011). Moreover, our findings add to recent remarkable demonstrations of applying decoding and time generalization methods to MEG (King and Dehaene, 2014; Tucciarelli et al., 2015; King et al., 2016; Wutz et al., 2016), and show a promising application of MVPA techniques to source level searchlight analysis with a focus on the temporal dynamics of conscious perception.

Acknowledgements

This work was supported by the European Research Council (WIN2CON, ERC StG 283404).

Author contributions

G.S. and N.W. conceived the approach. G.S., J.N.F. and M.F. implemented the experiment and collected the data. G.S. analyzed the data. G.S. and N.W. wrote the manuscript. All authors approved the current manuscript.

References

Ai L, Ro T (2014) The phase of prestimulus alpha oscillations affects tactile perception. J Neurophysiol 111:1300–1307.

Andersen LM, Pedersen MN, Sandberg K, Overgaard M (2016) Occipital MEG Activity in the Early Time Range (<300 ms) Predicts Graded Changes in Perceptual Consciousness. Cereb Cortex N Y N 1991 26:2677–2688.

Auksztulewicz R, Blankenburg F (2013) Subjective Rating of Weak Tactile Stimuli Is Parametrically Encoded in Event-Related Potentials. J Neurosci 33:11878–11887.

Auksztulewicz R, Spitzer B, Blankenburg F (2012) Recurrent Neural Processing and Somatosensory Awareness. J Neurosci 32:799–805.

658 Baars BJ (2005) Global workspace theory of consciousness: toward a cognitive
659 neuroscience of human experience. In: Progress in Brain Research, pp 45–53.
660 Elsevier.

661 Brainard D (1997) The Psychophysics Toolbox. Spat Vis:433–436.

662 Brancucci A, Lugli V, Perrucci MG, Gratta CD, Tommasi L (2014) A frontal but not parietal
663 neural correlate of auditory consciousness. Brain Struct Funct 221:463–472.

664 Chen T, Cai W, Ryali S, Supekar K, Menon V (2016) Distinct Global Brain Dynamics and
665 Spatiotemporal Organization of the Salience Network. PLOS Biol 14:e1002469.

666 Cichy RM, Khosla A, Pantazis D, Oliva A (2016) Dynamics of scene representations in the
667 human brain revealed by magnetoencephalography and deep neural networks.
668 NeuroImage Available at:
669 http://www.sciencedirect.com/science/article/pii/S1053811916300076 [Accessed
670 April 12, 2016].

671 Cichy RM, Pantazis D, Oliva A (2014) Resolving human object recognition in space and
672 time. Nat Neurosci 17:455–462.

673 Cichy RM, Ramirez FM, Pantazis D (2015) Can visual information encoded in cortical
674 columns be decoded from magnetoencephalography data in humans? NeuroImage
675 121:193–204.

676 Crick F, Koch C (2003) A framework for consciousness. Nat Neurosci 6:119–126.

677 Dagenbach D, Carr TH, Wilhelmsen A (1989) Task-induced strategies and near-threshold
678 priming: Conscious influences on unconscious perception. J Mem Lang 28:412–443.

679 Dehaene S, Changeux J-P (2011) Experimental and Theoretical Approaches to Conscious
680 Processing. Neuron 70:200–227.

681 Dehaene S, Changeux J-P, Naccache L, Sackur J, Sergent C (2006) Conscious,
682 preconscious, and subliminal processing: a testable taxonomy. Trends Cogn Sci
683 10:204–211.

684 Dehaene S, Charles L, King J-R, Marti S (2014) Toward a computational theory of conscious
685 processing. Curr Opin Neurobiol 25:76–84.

686 Devrim M, Demiralp T, Ademoglu A, Kurt A (1999) A model for P300 generation based on
687 responses to near-threshold visual stimuli. Cogn Brain Res 8:37–43.

688 Fallgatter AJ, Mueller TJ, Strik WK (1997) Neurophysiological correlates of mental imagery
689 in different sensory modalities. Int J Psychophysiol 25:145–153.

690 Felleman DJ, Essen DCV (1991) Distributed Hierarchical Processing in the Primate Cerebral
691 Cortex. Cereb Cortex 1:1–47.

692 Fisch L, Privman E, Ramot M, Harel M, Nir Y, Kipervasser S, Andelman F, Neufeld MY,
693 Kramer U, Fried I, Malach R (2009) Neural "Ignition": Enhanced Activation Linked to
694 Perceptual Awareness in Human Ventral Stream Visual Cortex. Neuron 64:562–574.

695 Foley JM, Legge GE (1981) Contrast detection and near-threshold discrimination in human
696 vision. Vision Res 21:1041–1053.

697 Frey JN, Ruhnau P, Leske S, Siegel M, Braun C, Weisz N (2016) The Tactile Window to
698 Consciousness is Characterized by Frequency-Specific Integration and Segregation
699 of the Primary Somatosensory Cortex. Sci Rep 6:20805.

700 Gordon EM, Laumann TO, Adeyemo B, Huckins JF, Kelley WM, Petersen SE (2016)
701 Generation and Evaluation of a Cortical Area Parcellation from Resting-State
702 Correlations. Cereb Cortex 26:288–303.

703 Gross J, Baillet S, Barnes GR, Henson RN, Hillebrand A, Jensen O, Jerbi K, Litvak V, Maess
704 B, Oostenveld R, Parkkonen L, Taylor JR, van Wassenhove V, Wibral M, Schoffelen
705 J-M (2013) Good practice for conducting and reporting MEG research. NeuroImage
706 65:349–363.

707 Haynes J-D, Sakai K, Rees G, Gilbert S, Frith C, Passingham RE (2007) Reading Hidden
708 Intentions in the Human Brain. Curr Biol 17:323–328.

709 Joos K, Gilles A, Van de Heyning P, De Ridder D, Vanneste S (2014) From sensation to
710 percept: The neural signature of auditory event-related potentials. Neurosci Biobehav
711 Rev 42:148–156.

712 Karns CM, Knight RT (2008) Intermodal Auditory, Visual, and Tactile Attention Modulates
713 Early Stages of Neural Processing. J Cogn Neurosci 21:669–683.

714 Kauramäki J, Jääskeläinen IP, Hänninen JL, Auranen T, Nummenmaa A, Lampinen J, Sams
715 M (2012) Two-Stage Processing of Sounds Explains Behavioral Performance

716 Variations due to Changes in Stimulus Contrast and Selective Attention: An MEG
717 Study. PLOS ONE 7:e46872.

718 King J-R, Dehaene S (2014) Characterizing the dynamics of mental representations: the
719 temporal generalization method. Trends Cogn Sci 18:203–210.

720 King J-R, Pescetelli N, Dehaene S (2016) Brain Mechanisms Underlying the Brief
721 Maintenance of Seen and Unseen Sensory Information. Neuron 92:1122–1134.

722 Kriegeskorte N, Goebel R, Bandettini P (2006) Information-based functional brain mapping.
723 Proc Natl Acad Sci U S A 103:3863–3868.

724 Kucyi A, Hodaie M, Davis KD (2012) Lateralization in intrinsic functional connectivity of the
725 temporoparietal junction with salience- and attention-related brain networks. J
726 Neurophysiol 108:3382–3392.

727 Lamme VAF (2006) Towards a true neural stance on consciousness. Trends Cogn Sci
728 10:494–501.

729 Langner R, Kellermann T, Boers F, Sturm W, Willmes K, Eickhoff SB (2011) Modality-
730 Specific Perceptual Expectations Selectively Modulate Baseline Activity in Auditory,
731 Somatosensory, and Visual Cortices. Cereb Cortex 21:2850–2862.

732 Lemus L, Hernández A, Luna R, Zainos A, Romo R (2010) Do Sensory Cortices Process
733 More than One Sensory Modality during Perceptual Judgments? Neuron 67:335–
734 348.

735 Leske S, Ruhnau P, Frey J, Lithari C, Müller N, Hartmann T, Weisz N (2015) Prestimulus
736 Network Integration of Auditory Cortex Predisposes Near-Threshold Perception
737 Independently of Local Excitability. Cereb Cortex 25:4898–4907.

738 Liang M, Mouraux A, Hu L, Iannetti GD (2013) Primary sensory cortices contain
739 distinguishable spatial patterns of activity for each sense. Nat Commun 4:1979.

740 Maris E, Oostenveld R (2007) Nonparametric statistical testing of EEG- and MEG-data. J
741 Neurosci Methods 164:177–190.

742 Melloni L, Schwiedrzik CM, Müller N, Rodriguez E, Singer W (2011) Expectations Change
743 the Signatures and Timing of Electrophysiological Correlates of Perceptual
744 Awareness. J Neurosci 31:1386–1396.

745 Menon V, Uddin LQ (2010) Saliency, switching, attention and control: a network model of
746 insula function. Brain Struct Funct 214:655–667.

747 Mulert C, Jäger L, Schmitt R, Bussfeld P, Pogarell O, Möller H-J, Juckel G, Hegerl U (2004)
748 Integration of fMRI and simultaneous EEG: towards a comprehensive understanding
749 of localization and time-course of brain activity in target detection. NeuroImage
750 22:83–94.

751 Naghavi HR, Nyberg L (2005) Common fronto-parietal activity in attention, memory, and
752 consciousness: Shared demands on integration? Conscious Cogn 14:390–425.

753 Nolte G (2003) The magnetic lead field theorem in the quasi-static approximation and its use
754 for magnetoencephalography forward calculation in realistic volume conductors.
755 Phys Med Biol 48:3637.

756 Oostenveld R, Fries P, Maris E, Schoffelen J-M, Oostenveld R, Fries P, Maris E, Schoffelen
757 J-M (2010) FieldTrip: Open Source Software for Advanced Analysis of MEG, EEG,
758 and Invasive Electrophysiological Data, FieldTrip: Open Source Software for
759 Advanced Analysis of MEG, EEG, and Invasive Electrophysiological Data. Comput
760 Intell Neurosci Comput Intell Neurosci 2011, 2011:e156869.

761 Oosterhof NN, Connolly AC, Haxby JV (2016) CoSMoMVPA: Multi-Modal Multivariate
762 Pattern Analysis of Neuroimaging Data in Matlab/GNU Octave. Front
763 Neuroinformatics:27.

764 Palva S, Linkenkaer-Hansen K, Näätänen R, Palva JM (2005) Early Neural Correlates of
765 Conscious Somatosensory Perception. J Neurosci 25:5248–5258.

766 Pernet CR, Latinus M, Nichols TE, Rousselet GA (2015) Cluster-based computational
767 methods for mass univariate analyses of event-related brain potentials/fields: A
768 simulation study. J Neurosci Methods 250:85–93.

769 Polich J (2007) Updating P300: An integrative theory of P3a and P3b. Clin Neurophysiol
770 118:2128–2148.

771 Pooresmaeili A, FitzGerald THB, Bach DR, Toelch U, Ostendorf F, Dolan RJ (2014) Cross-
772 modal effects of value on perceptual acuity and stimulus encoding. Proc Natl Acad
773 Sci 111:15244–15249.

774 Power JD, Cohen AL, Nelson SM, Wig GS, Barnes KA, Church JA, Vogel AC, Laumann TO,
775 Miezin FM, Schlaggar BL, Petersen SE (2011) Functional Network Organization of
776 the Human Brain. Neuron 72:665–678.

777 Ruhnau P, Hauswald A, Weisz N (2014) Investigating ongoing brain oscillations and their
778 influence on conscious perception – network states and the window to
779 consciousness. Conscious Res 5:1230.

780 Rutiku R, Martin M, Bachmann T, Aru J (2015) Does the P300 reflect conscious perception
781 or its consequences? Neuroscience 298:180–189.

782 Sandberg K, Andersen LM, Overgaard M (2014) Using multivariate decoding to go beyond
783 contrastive analyses in consciousness research. Conscious Res 5:1250.

784 Schurger A, Sarigiannidis I, Naccache L, Sitt JD, Dehaene S (2015) Cortical activity is more
785 stable when sensory stimuli are consciously perceived. Proc Natl Acad Sci
786 112:E2083–E2092.

787 Sergent C, Baillet S, Dehaene S (2005) Timing of the brain events underlying access to
788 consciousness during the attentional blink. Nat Neurosci 8:1391–1400.

789 Sergent C, Dehaene S (2004) Neural processes underlying conscious perception:
790 Experimental findings and a global neuronal workspace framework. J Physiol-Paris
791 98:374–384.

792 Smith FW, Goodale MA (2015) Decoding Visual Object Categories in Early Somatosensory
793 Cortex. Cereb Cortex N Y NY 25:1020–1031.

794 Smith SM, Nichols TE (2009) Threshold-free cluster enhancement: Addressing problems of
795 smoothing, threshold dependence and localisation in cluster inference. NeuroImage
796 44:83–98.

797 Tallon-Baudry C (2012) On the Neural Mechanisms Subserving Consciousness and
798 Attention. Front Psychol 2:397.

799 Tucciarelli R, Turella L, Oosterhof NN, Weisz N, Lingnau A (2015) MEG Multivariate
800 Analysis Reveals Early Abstract Action Representations in the Lateral
801 Occipitotemporal Cortex. J Neurosci 35:16034–16045.

802 Turella L, Tucciarelli R, Oosterhof NN, Weisz N, Rumiati R, Lingnau A (2016) Beta band
803 modulations underlie action representations for movement planning. NeuroImage
804 136:197–207.

805 Tzourio-Mazoyer N, Landeau B, Papathanassiou D, Crivello F, Etard O, Delcroix N, Mazoyer
806 B, Joliot M (2002) Automated Anatomical Labeling of Activations in SPM Using a
807 Macroscopic Anatomical Parcellation of the MNI MRI Single-Subject Brain.
808 NeuroImage 15:273–289.

809 Van Essen DC, Drury HA, Dickson J, Harwell J, Hanlon D, Anderson CH (2001) An
810 Integrated Software Suite for Surface-based Analyses of Cerebral Cortex. J Am Med
811 Inform Assoc 8:443–459.

812 van Gaal S, Lamme VAF (2012) Unconscious High-Level Information Processing:
813 Implication for Neurobiological Theories of Consciousness. The Neuroscientist
814 18:287–301.

815 Veen BDV, Drongelen WV, Yuchtman M, Suzuki A (1997) Localization of brain electrical
816 activity via linearly constrained minimum variance spatial filtering. IEEE Trans
817 Biomed Eng 44:867–880.

818 Wühle A, Mertiens L, Rüter J, Ostwald D, Braun C (2010) Cortical processing of near-
819 threshold tactile stimuli: An MEG study. Psychophysiology 47:523–534.

820 Wutz A, Muschter E, van Koningsbruggen MG, Weisz N, Melcher D (2016) Temporal
821 Integration Windows in Neural Processing and Perception Aligned to Saccadic Eye
822 Movements. Curr Biol 26:1659–1668.

823 Wyart V, Tallon-Baudry C (2008) Neural Dissociation between Visual Awareness and Spatial
824 Attention. J Neurosci 28:2667–2679.

825 Zoefel B, Heil P (2013) Detection of Near-Threshold Sounds is Independent of EEG Phase
826 in Common Frequency Bands. Front Psychol 4:262.

827
828
829
830